0031-3998/05/5703-0384
PEDIATRIC RESEARCH

Vol. 57, No. 3, 2005
Printed in U.S.A.

Alveolarization in Retinoic Acid Receptor-β–Deficient Mice

JEANNE M. SNYDER, MELINDA JENKINS-MOORE, SHEILA K. JACKSON, KELLI L. GOSS, HUI-HUI DAI, PETER J. BANGSUND, VINCENT GIGUERE, AND STEPHEN E. MCGOWAN

Departments of Anatomy and Cell Biology [J.M.S., M.J.-M., K.L.G., P.J.B.] and Internal Medicine [S.K.J., H.-H.D., S.E.M.], University of Iowa College of Medicine, Iowa City, IA 52242; Veterans Affairs Research Service [S.K.J., H.-H.D., S.E.M.], Iowa City, IA 52242; and Department of Biochemistry [V.G.], McGill University, Montreal, Quebec, Canada H3A 1A1

ABSTRACT

Retinoids bind to nuclear receptors [retinoic acid receptors (RARs) and retinoid X receptors]. RARβ, one of three isoforms of RARs (α, β, and γ), is expressed in the fetal and adult lung. We hypothesized that RARβ plays a role in alveolarization. Using morphometric analysis, we determined that there was a significant increase in the volume density of airspace in the alveolar region of the lung at 28, 42, and 56 d postnatal age in RARβ null mice when compared with wild-type controls. The mean cord length of the respiratory airspaces was increased in RARβ null animals at 42 d postnatal age. Respiratory gas-exchange surface area per unit lung volume was significantly decreased in RARβ null animals at 28, 42, and 56 d postnatal age. In addition, alveolar ducts tended to comprise a greater proportion of the lung airspaces in the RARβ null mice. The RARβ null mice also had impaired respiratory function when compared with wild-type control mice. There was no effect of RARβ gene deletion on lung platelet-derived growth factor (PDGF) receptor α mRNA levels in postnatal lung tissue at several postnatal ages. However PDGF-A protein levels were significantly lower in the RARβ null mice than in wild-type controls. Thus, deletion of the RARβ gene impairs the formation of the distal airspaces during the postnatal phase of lung maturation in mice *via* a pathway that may involve PDGF-A. **(*Pediatr Res* 57: 384–391, 2005)**

Abbreviations

BrdU, bromodeoxyuridine
Lm, mean cord length
MV, minute volume
PDGF, platelet-derived growth factor
PDGF-Rα, platelet-derived growth factor receptor α
R, respiratory rate
RAR, retinoic acid receptor
RXR, retinoid X receptor
TV, tidal volume

Retinoids regulate the development of the conducting airways and the gas-exchange portion of the lung (1). The major biologically active retinoid, all-trans retinoic acid, is a metabolite of retinol (vitamin A) (2). Retinol can be stored within lung tissue esterified to fatty acids, where it can be released by retinyl ester hydrolases and then be converted to all-trans retinoic acid (1). All-trans retinoic acid binds with high affinity to retinoic acid receptors (RARs), which exist in three isoforms, α, β, and γ (3). Retinoid X receptors (RXRs) primarily bind 9-cis retinoic acid (3). RARs form a heterodimer with RXRs and bind to retinoid responsive elements in target genes (3). RARs and RXRs are members of the steroid hormone receptor superfamily of transcription factors (3).

Massaro and co-workers (4,5) reported that all-trans retinoic acid increases the number of alveoli in rat lung. In the first study, postnatal rats that were treated with all-trans retinoic acid had increased numbers of alveoli and increased gas exchange surface area (4). A synthetic glucocorticoid, dexamethasone, decreases the number of alveoli in this animal model. All-trans retinoic acid overcame the inhibitory effects of dexamethasone on alveolarization in the postnatal rats (4). In the second study, elastase was insufflated into the lungs of adult rats to create a model of emphysema, *i.e.* the damaged lungs in the treated rats were characterized by fewer and larger alveoli and decreased gas exchange area (5). When the elastase-treated rats received an injection of all-trans retinoic acid, the emphysema-like effects of the elastase treatment were almost completely reversed, *i.e.* the number of alveoli was increased, the size of the alveoli was reduced, and the alveolar gas-exchange surface area was similar to that in control animals, which did not receive elastase (5). Together, the results of these studies are suggestive that all-trans retinoic acid regulates the forma-

Received April 23, 2004; accepted August 2, 2004.
Correspondence: Jeanne M. Snyder, Ph.D., Department of Anatomy and Cell Biology, 1-550 Bowen Science Building, Iowa City, IA 52242; e-mail: jeanne-snyder@uiowa.edu
This work was supported by National Institutes of Health Grants HL62861, HL53430, and DERC DK-25295 and a grant from the March of Dimes Birth Defects Foundation.

DOI: 10.1203/01.PDR.0000151315.81106.D3

tion of alveoli in postnatal and adult rat lung. More recently, two groups of investigators reported that retinoic acid fails to reverse elastase-induced emphysema in adult mice (6,7).

In a previous study, we showed that alveolarization in postnatal RARγ gene-deleted mice is impaired (8). Alveolar formation is also impaired in RARα gene-deleted mice (9). In the present study, we hypothesized that all-trans retinoic acid also binds to RARβ in the lung and that activated, ligand-bound RARβ in turn directly or indirectly regulates genes that promote alveolarization. Massaro *et al.* (10) reported that RARβ gene-deleted mice have smaller and more numerous alveoli in their lungs; however, alveolar surface area was not different between the control and RARβ null mice. In the present study, we evaluated the effects of RARβ gene deletion on morphologic, biochemical, and physiologic aspects of alveolarization in the neonatal mouse lung. Our results suggest that RARβ, along with RARγ and RARα, plays a role in postnatal lung alveolarization.

METHODS

RARβ gene-deleted mice were provided by Dr. Vincent Giguere (McGill University, Montreal, Quebec) and were bred at the Animal Research Facility at the Iowa City Veterans Affairs Medical Center, following a protocol approved by the Animal Research Review Committee at the University of Iowa. The targeted disruption of the RARβ gene in these mice has been described previously (11). The resultant line is in a C57BL6, 129/SV+/C+ background. The life span of the RARβ null mice does not differ from that of control, wild-type mice and is ~1.5–2.0 y (11). With the use of Northern blot analysis and an exon 6 cDNA probe, no RARβ mRNA transcripts were detected in the RARβ null mice (11). The mice were fed Harlan Teklab 7001 mouse chow and water *ad libitum*. Initially, male and female mice that were heterozygous for the RARβ mutation were bred to obtain wild-type and homozygous RARβ gene-deleted animals. Genotypes were confirmed using Southern blot analysis. The cDNA probe used to detect the mouse RARβ gene was derived from intron 5 immediately 5' to the neomycin resistance gene insertion site and hybridized to bands that were 5.2 and 6.0 kb for the wild-type and RARβ null mice, respectively (11). The RARβ null mice used in these studies were derived from mating homozygous null male and female mice. Control, wild-type animals were derived from the same strain of mice and were progeny of matings of the heterozygous RARβ mice that were used to produce the parental RARβ null mice. Litter size did not vary between the wild-type and RARβ matings. Animals were killed on various postnatal days, and their body weights and lung volumes were recorded. Approximately 12 litters of wild-type and 12 litters of RARβ matings were used in this study. For some protocols, a portion of the lung was immediately frozen in liquid nitrogen and stored at −70°C. Tissues that were collected from the wild-type and RARβ animals were used for one type of measurement, except for the mice that were used for the CO uptake study, which were also used in the pressure-volume studies.

Morphologic studies. For morphologic studies, the anterior chest wall was removed and the lungs were perfused with 2% paraformaldehyde in 0.1 M of sodium phosphate buffer (pH 7.0) *via* the right ventricle of the heart. The trachea was cannulated, and the cannula was tied firmly in place. The lungs then were filled through the trachea with 2% paraformaldehyde at 20 cm H_2O pressure and were maintained at this pressure for 18 h at 4°C. This inflation pressure has been used in previous studies describing the influence of retinoids on alveolarization (4,5,10). The lungs were monitored for leakage during this procedure, and only lungs that did not leak were used for further study. After fixation, the lungs were removed from the chest cavity, and the heart and mediastinal tissues were removed. The lungs were dehydrated and embedded in paraffin. Sections (3.5-μm thickness) were mounted on glass slides, deparaffinized, and stained with hematoxylin and eosin. Some sections were deparaffinized, then stained immunohistochemically for RARβ. Briefly, for immunostaining, sections were hydrated in PBS, the endogenous peroxidase activity was quenched with 0.3% H_2O_2, and the sections were blocked with 1% horse serum. Sections then were incubated with the primary antibody (rabbit anti-human RARβ; Upstate Biochemical, Albany, NY; 1:1000) for 1 h at room temperature. The sections then were stained with a Vectastain Elite kit using the manufacturer's directions (Vector Laboratories, Burlingame, CA). Positive staining was visualized by incubation in diaminobenzidine substrate (3%) followed by counterstaining with hematoxylin.

Morphometry. Randomly chosen paraffin blocks of right lower lobe lung tissue that was obtained from wild-type and RARβ null mice were sectioned and then stained with hematoxylin and eosin. Wild-type and RARβ null mice were studied at 0, 12, 28, 42, and 56 d postnatal age. Sections (two per mouse) were chosen at random, and six randomly selected microscopic fields of respiratory airspaces (alveoli, alveolar sacs, and ducts) from the lung sections were photographed at ×200. The photographs were uniformly enlarged, overlaid with transparent grids, and analyzed using morphometric methods (12). The volume densities of airspace and tissue were determined by point counting using a 10 × 10 grid with 100 evenly spaced points, ~42 μm apart, as described previously (8). A further analysis of the 28-, 42-, and 56-d-old samples was conducted to measure the volume density of the airspace occupied by alveoli *versus* alveolar ducts and sacs as described by Kawakami *et al.* (13). Alveoli were considered to be the smallest airspaces encompassed by alveolar wall tissue or by an imaginary straight line drawn across their opening into an alveolar duct or sac. Alveolar ducts and sacs refer to the cylindrical core of airspace that was internal to the openings of alveoli. Mean cord lengths (Lm) were determined by counting intersections of airspace walls (including alveoli, alveolar sacs, and alveolar ducts) with an array of 70 lines, each ~33 μm long (8). The Lm is an estimate of the distance from one airspace wall to another airspace wall. The star volume method was used to calculate the volume of individual alveoli (14,15). A system of 48 evenly spaced test points (crosses) was superimposed on each photograph in a random orientation. Test points that fell within the airspace of an alveolus or within airspace in an alveolar duct or alveolar sac were used to mark airspace structures that were analyzed further. The distance from one wall of the marked airspace to the opposite wall was measured using a ruler in the same orientation as the horizontal portion of the cross on the transparent grid. This dimension is the point-sampled intercept (1) and was used to calculate the volume of the individual airspaces using the formula $l^3\pi/3$. An average of 34 alveoli and 19 alveolar ducts or sacs were measured per animal. The grids used for morphometry were enlarged from those described previously (12). All morphometric measurements were made by two or three independent observers who were unaware of the genotypes of the animals being analyzed. Several animals were analyzed per condition, and at least six photographs were analyzed per animal. The volume densities of the airspace and tissue, the Lm, and the alveolar surface area were calculated as described previously (8). Surface areas are expressed per cm^3 of distal lung tissue. Means and SEMs were calculated for each condition, and statistical comparisons were performed using ANOVA and unpaired *t* test (16). To estimate the sampling error in our morphometric measurements, we calculated the SEM expressed as a percentage of the mean. For the volume density of airspace data, this parameter varied from ~1 to 4.7% (mean 2.7%). For the volume density of tissue data, this parameter varied from 2.1 to 11.3% (mean 6%).

Bromodeoxyuridine labeling. At postnatal days 4, 7, 12, and 16, wild-type and RARβ null mice received 10 mg of bromodeoxyuridine (BrdU) per 100 g of body weight *via* an intraperitoneal injection 4 h before being killed. After fixation, paraffin embedding, and sectioning of the lung tissue as described above, randomly chosen sections were deparaffinized, hydrated, and then incubated for 30 min in 0.5% H_2O_2 in 0.05 M of NaH_2PO_4 and 0.05 M of $(Na)_3$ citrate (pH 5.5). After washing three times with PBS, the sections were incubated for 1 h in 2 N of HCl, and the HCl then was neutralized by washing twice with 0.1 M of Na borate (pH 8.5) and then with 50 mM of Tris-HCl (pH 7.5) and 2 mM of EDTA. The sections then were incubated for 10 min at 25°C in 0.125 mg/mL of Pronase E in 50 mM of Tris-HCl (pH 7.5) and 2 mM of EDTA and rinsed once with PBS that containing 2 mg/mL of glycine. The sections next were incubated at 4°C overnight in 7.5 U/mL of mouse-anti BrdU antibody (Roche Biochemicals, Indianapolis, IN) diluted in PBS that contained 0.2% Tween-20, 0.5% BSA, and 2% normal goat serum. The sections then were rinsed three times for 10 min each with PBS plus 0.5% BSA and once with PBS. The peroxidase-conjugated antibody was localized using a diaminobenzidine substrate as described above. The peroxidase-containing cells in alveoli were distinguished from cells that were located in airways and blood vessels and enumerated using a microscope at ×200 magnification. At least 300 cells per section were counted; conducting airway and blood vessel cells were excluded from the 300 cells. Sections from three wild-type and 3 RARβ null mice were used for the 4-, 10-, and 12-d time points. At 7 d, four animals per condition were used. At 16 d, two animals per condition were used.

Respiratory mechanics. At postnatal age 56 d, mice were weighed and placed in the 100-mL restrainer of a Tidal Volume Meter (Columbus Instruments, Columbus, OH). The head was placed and sealed in the nose cone with a pneumatic collar, and the pressure inside the restrainer was monitored with a pressure transducer that was connected to a digital-to-analog converter. Respiratory rate (R), tidal volume (TV), and minute volume (MV) were monitored until stable, and then eight readings were made. The mean R, TV,

and MV were calculated from the eight repeated readings. CO uptake was monitored using a CO Uptake Monitor (Columbus Instruments) and 0.2% CO. The instrument was calibrated on the day of the study using a certified mixture of 2000 ppm of CO with the balance as air. The animals were confined to a 250-mL compartment during the measurement but were otherwise unrestrained. The respiratory rate was monitored during the measurement of CO uptake. The mice were exposed to the CO for 2 min, and the chamber was quickly purged with air and the animal was removed. The CO uptake measurements were normalized to the MV that was determined for the same animal immediately before the CO uptake measurement. The mice then were anesthetized with 100 mg/kg of ketamine and 15 mg/kg of xylazine. A tracheostomy was performed, and a 20-G cannula was inserted into the trachea and tied in place. This was attached to a constant volume ventilator (Harvard Apparatus, Cambridge, MA), and the lung was ventilated for 5 min with 100% oxygen to purge the N_2. The cannula was plugged, and the O_2 was allowed to absorb from the lung while the blood continued to circulate, thereby inducing complete atelectasis. The thoracic cavity was opened, and the anterior chest wall was carefully resected. The lateral chest wall was cut, and the diaphragm was retracted caudally to allow full expansion of the lungs without impediment from the chest wall. The lung was gradually inflated to 30 cm H_2O pressure and deflated in 100-μL increments using a Harvard PHD 2000 programmable syringe pump. Pressure was measured using a Validyne Model DP45-28 pressure transducer. The signal was conditioned by a Validyne carrier-demodulator and sent to a Kipp and Zonen strip-chart recorder. The transducer was calibrated using a water manometer. The compliance measurements were made within 15 min after the heart stopped, and lungs with leaks were excluded from the analysis. The volume-pressure data were expressed as described previously (17).

Analysis of platelet-derived growth factor receptor α mRNA. Total RNA was isolated from whole lung tissue obtained at 0, 6, 10, 12, and 16 d postnatal age using RNAzol as described previously (18). Ribonuclease protection analysis was used to quantify the steady-state levels of the platelet-derived growth factor receptor α (PDGF-Rα) mRNA in lung tissue from wild-type and RARβ null mice at various postnatal ages. The mouse PDGF-Rα cDNA was prepared from pMaRKS by removing the portion of the cDNA 3' to the *Psh*A1 site and the attached 1 phage DNA (19). This left the 3' terminus of the cDNA proximal to the T7 promoter that was used to transcribe the plasmid after it had been linearized by restriction with *Stu*I. Antisense cRNAs for PDGFR-α and for cyclophilin were synthesized using T7 viral RNA polymerase and an *in vitro* transcription kit from Boehringer-Mannheim (Indianapolis, IN). The transcripts were subjected to denaturing PAGE, and the full-length transcripts were excised from the gel and eluted (19). The ribonuclease protection analysis was performed using the method described previously and the protected [^{32}P]-cRNA was resolved on 4%, 0.4-mm-thickness denaturing polyacrylamide gels (20). Yeast tRNA was used as a control for hybridization to RNA in a sequence-independent manner. Under the hybridization and RNase treatment conditions that were used, the yeast tRNA did not protect the probes from digestion. The gels were dried, and autoradiograms were prepared and subjected to densitometry (20). The size of the protected PDGF-Rα mRNA was 440 bp. The quantity of the protected cRNA was normalized to the quantity of cyclophilin mRNA for the corresponding RNA sample to account for differences in the quantities of RNA that were assayed (19).

Immunoblotting for PDGF-A protein. Lung tissue collected at 28 d postnatal age from wild-type and RARβ null mice was homogenized in sterile water that contained phenylmethylsulfonyl fluoride (1 mM), and the homogenates were centrifuged at 600 $\times$ *g* for 10 min at 4°C. The supernatants were collected, and the protein concentrations were measured using the method of Bradford (21). A total of 100 μg of total protein from each homogenate was separated on a 10% polyacrylamide minigel (BioRad), then transferred electrophoretically to Immobilon membrane (Millipore, Bedford, MA). Membranes were incubated in rabbit anti–PDGF-A antibodies (Santa Cruz Biotechnologies, Santa Cruz, CA; 1:500), rinsed, then incubated in a secondary antibody as previously described (22). The immunoreactive protein was visualized by enhanced chemiluminescence (Amersham Life Sciences-USB, Arlington Heights, IL). The relative amount of PDGF-A protein was semiquantified by densitometry and expressed relative to levels in wild-type mice.

RESULTS

RARβ was present in the nucleus of alveolar cells in wild-type control mouse lung tissue (Fig. 1). Many of the positively stained cells seemed to be alveolar type II cells on the basis of their cuboidal shape, round nucleus, and location in the corner of the alveoli. In contrast, no RARβ immunostaining was detected in lung tissue obtained from RARβ gene-deleted

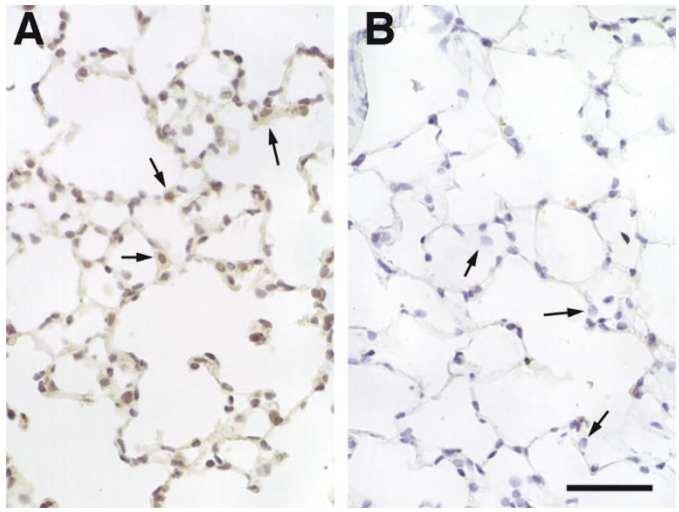

Figure 1. RARβ immunostaining. In wild-type mice, RAR-β staining was primarily detected in the nuclei of alveolar cells. Many of the positively stained cells appeared to be alveolar type II cells (arrows) (A). No specific RAR-β immunostaining was present in lung tissue obtained from the RARβ null mice (B). Bar indicates 50 μm.

mice. Similar results were obtained with immunoblot analysis, *i.e.* an immunoreactive band of ~50 kD was detected in homogenates of wild-type lung tissue, but no corresponding band was detected in homogenates of lung tissue from the RARβ null mice (data not shown).

Body weights (in grams) at 0 and 12 d postnatal age did not differ between the wild-type controls and RARβ null animals (day 0: wild-type = 1.6 $\pm$ 0.1 and RARβ null = 1.8 $\pm$ 0.1; day 12: wild-type = 6.3 $\pm$ 0.4 and RARβ null = 7.2 $\pm$ 0.3). At 28 d postnatal age, the body weights of the RARβ null animals were slightly but significantly lower than those of wild-type control mice (18.1 $\pm$ 0.3 wild type and 15.5 $\pm$ 0.6 RARβ null; $p < 0.05$). However, at 42 and 56 d postnatal age, there was no difference in the body weights of the two groups of animals (42 and 56 d: wild-type = 20.1 $\pm$ 1.3 and 25.2 $\pm$ 0.3, respectively; RARβ null = 21.1 $\pm$ 0.2 and 25.1 $\pm$ 0.8, respectively). There was no difference in either the lung volumes or the ratio of the lung volume to body weight between the RARβ null mice and the control, wild-type mice at 28, 42, and 56 d postnatal age (data not shown). It was not possible to measure accurately lung volumes by displacement at 0 and 12 d postnatal age. There was no significant effect of the sex of the animal on the body weight or lung volume variables.

The morphology of distal lung tissue at postnatal day 0 (the day of birth) did not seem to differ between the wild-type and RARβ gene-deleted mice (Fig. 2*A* and *B*). In the mouse, alveolarization is primarily a postnatal event, largely occurring within the first 2 postnatal wk but continuing until ~6 wk of age (23). When lung tissue collected at 56 d postnatal age was examined, there seemed to be a greater proportion of alveolar ducts in lung of the RARβ null mice when compared with wild-type lung tissue (Fig. 2*C* and *D*).

There were no significant differences in the volume densities of the airspace or tissue at the 0- or 12-d postnatal age time points when the control and RARβ null lung tissues were compared (data not shown). In contrast, the volume density of

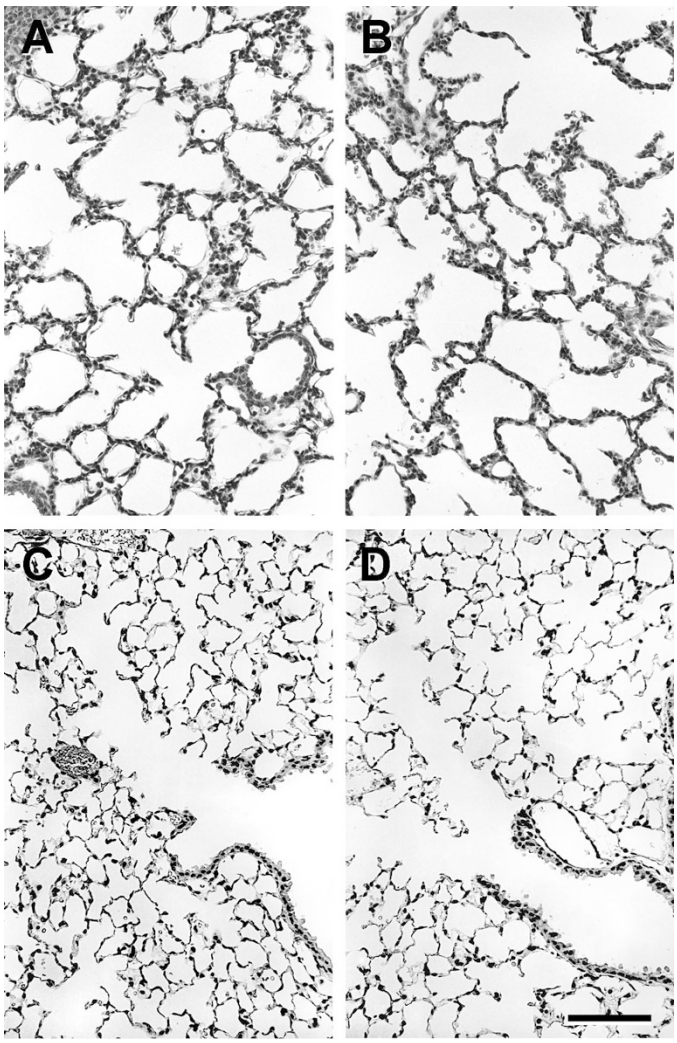

Figure 2. Light micrographs of lung tissue obtained from wild-type and RARβ null mice at 0 and 56 d postnatal age. (*A*) Wild-type lung, 0 d postnatal age. (*B*) RARβ null lung, 0 d postnatal age. (*C*) Wild-type lung, 56 d postnatal age. (*D*) RARβ null lung, 56 d postnatal age. There was no obvious difference in lung structure between the wild-type and RARβ gene-deleted mice at the 0-d postnatal age time point. However, at 56 d of age, the lung tissue in the RARβ null mice seemed to have less gas-exchange surface area and a greater proportion of alveolar ducts and sacs. Bar = 100 μm.

airspace in the distal lung was significantly greater in lung from RARβ null mice than in lung from wild-type mice at the 28-, 42-, and 56-d postnatal time points (Table 1). Conversely, the volume density of tissue was significantly lower in the lung from RARβ null mice than in lung from control animals at the 28- and 42-d postnatal time points (Table 1). The Lm of air spaces declined as a function of postnatal age in both wild-type and RARβ null mice (Table 1). There was no significant difference between the two conditions in the Lm at any time point studied except at 42 d postnatal age, when it was significantly greater in the RARβ null animals when compared with wild-type controls. However, there was a trend for the Lm to be slightly larger in the RARβ null mice at the 28-, 42-, and 56-d postnatal age time points (Table 1). At 28, 42, and 56 d postnatal age, the gas-exchange surface area per cm^3 of lung tissue was decreased by ~30% in the RARβ null mice when compared with the wild-type control mice (Table 1). The mean volume of alveoli and number of alveoli were determined at 28, 42, and 56 d postnatal age (Table 1). There was no significant difference in the mean volume of individual alveoli at any age in the wild-type mice *versus* the RARβ null mice (Table 1). The number of alveoli per cm^3 of lung tissue also did not differ between the wild-type and RARβ null mice (Table 1). The distribution of alveolar volumes likewise did not differ significantly between the wild-type and RARβ null mice (Fig. 3). However, we did find that alveolar ducts and alveolar sacs comprise a significantly greater proportion of the tissue in the RARβ null mice at 28, 42, and 56 d postnatal age (Fig. 4).

We evaluated CO uptake and pressure/volume characteristics in wild-type and RARβ null mice at 56 d postnatal age to ensure that the animals were large enough to obtain accurate measurements (Fig. 5). CO uptake was significantly reduced in the RARβ null mice when compared with wild-type mice at 56 d postnatal age (Fig. 5*A*). The pressure/volume characteristics of the lung were not significantly altered at the 56-d postnatal age time point (data not shown).

Evaluation of BrdU labeling, used to identify dividing cells, revealed that there was no difference in the proportion of labeled cells in the distal, alveolar region of the lungs, excluding blood vessels and conducting airways, in wild-type *versus* RARβ null mice during the period of peak alveolarization [days 4 to 16 (Fig. 6)]. The proportion of labeled cells was highest at the earliest time point (4 d postnatal age) and declined thereafter to essentially zero at 16 d postnatal age (Fig. 6). There was no significant difference in the thickness of the alveolar walls in wild-type *versus* RARβ null mice at any of the time points examined in this study (Fig. 7).

Animals in which the PDGF-A gene is deleted have impaired lung septation and alveolarization in the postnatal period

Table 1. *Morphometry of lung tissue from wild-type and RARβ null mice*

	4 Weeks postnatal		6 Weeks postnatal		8 Weeks postnatal	
Parameter	Wild type	RARβ null	Wild type	RARβ null	Wild type	RARβ null
n	4	5	3	4	5	5
Airspace volume density (%)	0.67 ± 0.01	0.72 ± 0.01*	0.68 ± 0.02	0.74 ± 0.01*	0.64 ± 0.02	0.71 ± 0.01*
Tissue volume density (%)	0.33 ± 0.01	0.28 ± 0.01*	0.32 ± 0.02	0.26 ± 0.02*	0.33 ± 0.03	0.29 ± 0.01
LM (μm)	36.4 ± 2.3	41.4 ± 1.7	30.2 ± 0.6	36.4 ± 1.5*	29.0 ± 1.1	32.3 ± 1.3
Surface area (cm^2 per cm^3)	344.6 ± 19.3	248.8 ± 20.1*	443.3 ± 30.1	271.3 ± 17.2*	489.5 ± 46.8	359.1 ± 14.2*
Alveolar volume ($\mu m^3 \times 10^4$)	5.09 ± 0.50	5.70 ± 0.33	4.19 ± 0.92	5.47 ± 0.88	4.19 ± 0.95	3.69 ± 0.26
No. of alveoli per cm^3 Lung ($\times 10^6$)	8.60 ± 0.85	7.92 ± 0.44	11.82 ± 1.98	9.39 ± 1.24	12.38 ± 3.10	12.61 ± 0.99

Data are mean ± SEM.

* $p < 0.05$ *vs* wild-type condition at the same age, unpaired *t* test.

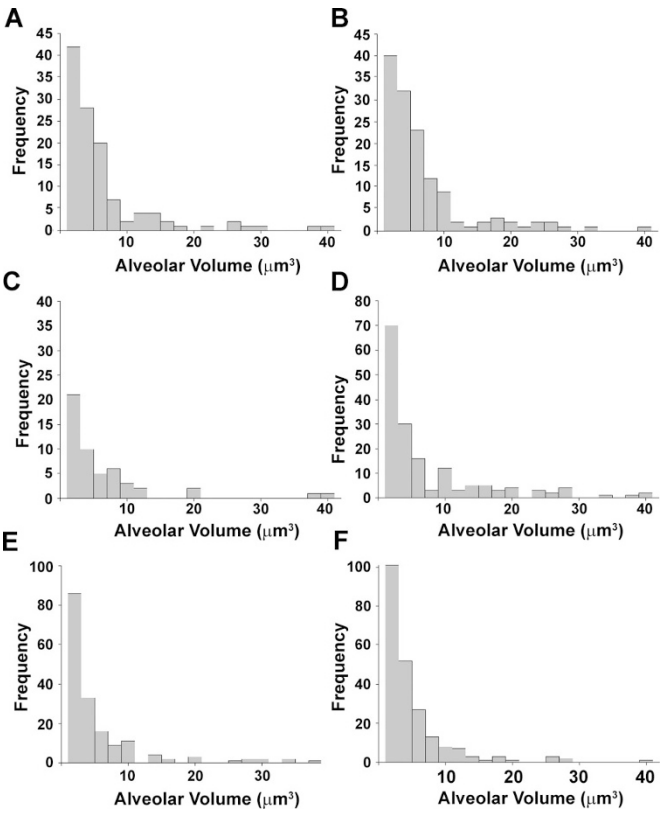

Figure 3. Frequency distribution of alveolar volumes in wild-type and RARβ null mice. The volume of individual alveoli was measured in wild-type mice at 4 wk (*A*), 6 wk (*C*) and 8 wk (*E*). and in RARβ null mice at 4 wk (*B*), 6 wk (*D*), and 8 wk (*F*). There was no difference in the distribution of alveolar volumes as determined by χ^2 analysis.

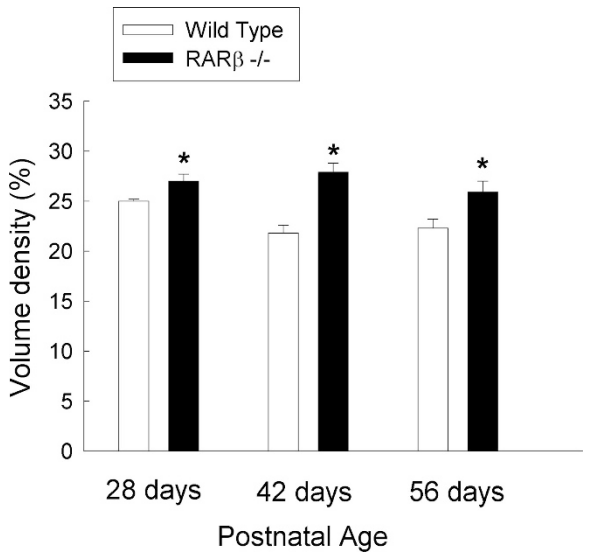

Figure 4. Morphometric analysis of the volume density occupied by alveolar duct air and alveolar sac air in lung tissue obtained from wild-type and RARβ null mice at 28, 42, and 56 d postnatal age (n = 3–5 for each condition). The data are expressed as percentage of volume density. Alveolar ducts and sacs occupied a significantly greater proportion of the lung tissue in the RARβ null mice (*$p < 0.05$, unpaired t test).

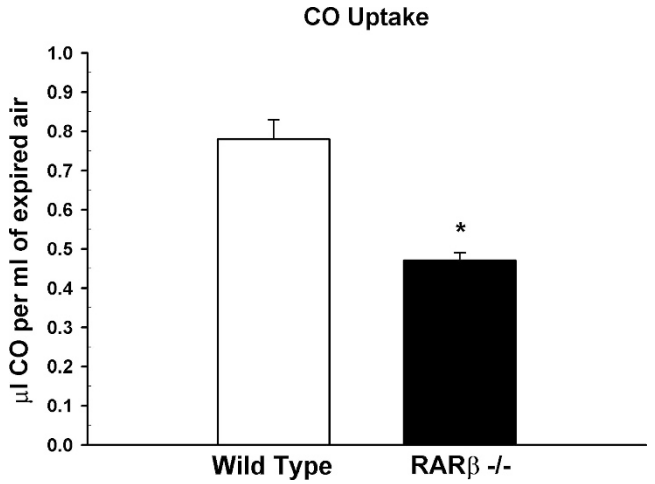

Figure 5. Physiologic function in wild-type *vs* RARβ null mice. (*A*) CO uptake. At 56 d postnatal age, the RARβ null mice (n = 6) had significantly decreased CO uptake when compared with wild-type mice (n = 6). The data are expressed as μl of CO taken up per ml of expired air (*$p < 0.05$, t test).

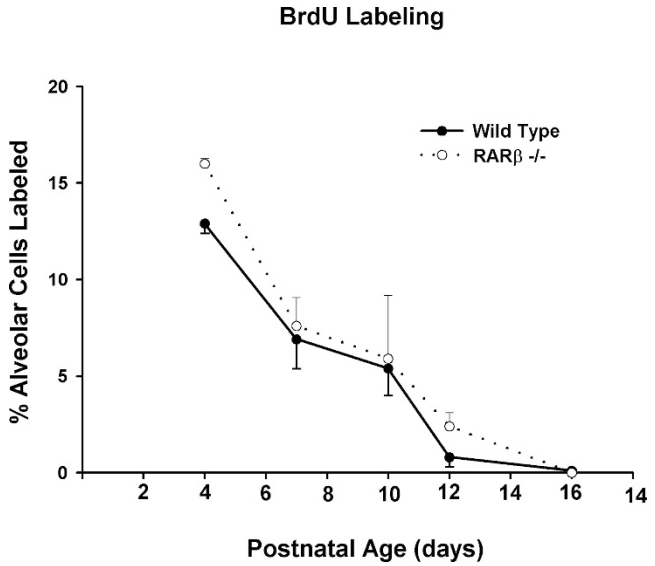

Figure 6. BrdU incorporation by nuclei of alveolar cells. Postnatal wild-type and RARβ null mice received an injection of BrdU to evaluate cell division in the distal lung gas-exchange tissue. The data are expressed as the percentage of alveolar cells that were BrdU labeled. There was no difference between the wild-type and RARβ null mice in the percentage of BrdU-labeled cells in the alveolar region at any of the postnatal time points examined.

(24,25). PDGF-Rα binds PDGF-A dimers (24,25). Therefore, PDGF-A protein and PDGF-Rα mRNA levels were evaluated in wild-type *versus* RARβ null mice. Mouse lung PDGF-A migrated at ~34 kD (Fig. 8 insert). There was a significant decrease in the relative amount of PDGF-A in the lung tissue from RARβ gene-deleted mice when compared with levels in wild-type mice (Fig. 8). Measurements of PDGF-Rα mRNA levels made at 0-, 6-, 10-, 12-, and 16-d postnatal time points revealed no significant difference in the relative amount of PDGF-Rα mRNA in lung tissue obtained from wild-type control *versus* RARβ null mice at any time point examined. In addition, the levels of PDGF-Rα mRNA remained relatively level during this period (data not shown).

DISCUSSION

There are three isoforms of RARs in the mouse: α, β, and γ (3,26). Until recently, no abnormal lung phenotype had been

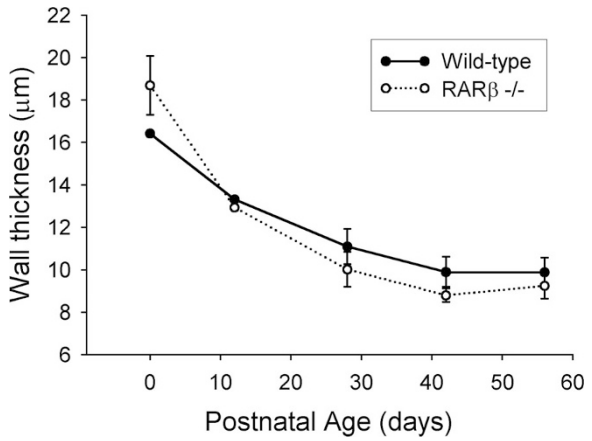

Figure 7. Wall thickness in wild-type and RARβ null mice at several postnatal ages. The thickness of the walls of alveoli, alveolar sacs, and alveolar ducts declined over time in both wild-type and RARβ null mice ($n = 3$–5 per condition). There was no significant difference in wall thickness in the wild type *vs* the RARβ null mice at any time point.

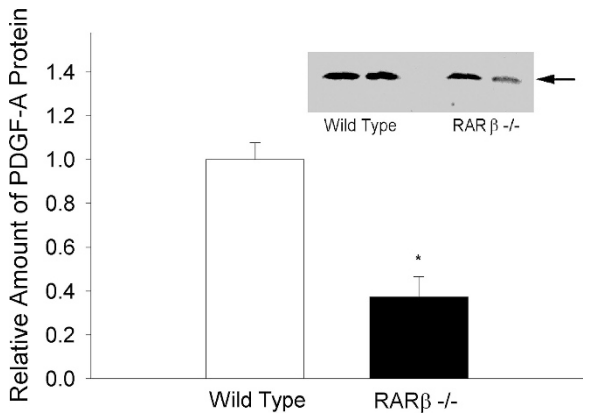

Figure 8. PDGF-A protein in lungs of wild-type *vs* RARβ null mice. Densitometric data for PDGF-A protein present in lung tissue obtained from wild-type animals ($n = 6$) and RARβ null animals ($n = 6$), all at 28 d postnatal age. There was a significant decrease in the PDGF-A content of the RARβ null lung tissue when compared with wild-type controls (*$p < 0.05$, unpaired t test). (*Insert*) Representative immunoblot for PDGF-A in lung tissue from two wild-type and two RARβ null mice at 28 d postnatal age. The immunoreactive PDGF-A migrated at ~34 kD (*arrow*).

associated with deletion of any of these genes (8,10,27). However, others have shown that simultaneous deletion of RARα and RARβ produces pulmonary hypogenesis or agenesis, which is usually unilateral (28). Some investigators have speculated that the three RAR isoforms are redundant and that deletion of only one RAR isoform may have minor effects because the RAR isoforms that are still present may replace the deleted RAR isoform (3). However, data from RARγ gene-deleted mice suggest that there may be specific lung abnormalities that are associated with deletion of an individual RAR gene (8). The RARγ null mice were characterized by decreased elastin content, decreased alveolar number, and an increase in the Lm of alveoli at 4 wk of age (6). In addition, it was reported recently that RARα gene-deleted mice have decreased alveolar surface area and decreased numbers of alveoli when compared with wild-type controls (9). It is interesting that the effect of the RARα gene deletion is not apparent until 50 d postnatal age (9).

RARβ is expressed in the fetal and adult lung (29). RARβ may play a role in branching morphogenesis in early stages of fetal lung development (30). More recently, it was reported that RARβ2 and RARβ4 mRNAs are present in postnatal mouse lung tissue, with the highest levels occurring at postnatal days 1–15, when levels are several times greater than in adult lung tissue (31). *In situ* hybridization showed that the RAR mRNA was expressed in alveolar regions of the lung (31). Yang *et al.* (32) showed that overexpression of a dominant negative RAR in the postnatal lung on days 1–21 after birth resulted in larger alveoli, fewer alveoli, fewer alveolar epithelial cells, and decreased alveolar surface area in the treated mice. These results suggest that RARs are required for postnatal alveolarization in the mouse lung. In the present study, RARβ was detected in alveolar epithelial cells. We observed significantly decreased tissue volume density and decreased gas-exchange surface area in RARβ gene-deleted animals. Because no morphologic effects of the RARβ gene deletion were observed in lung harvested at the day of birth or at postnatal day 12, the results of the altered developmental processes in the RARβ null mice apparently become manifest during later postnatal lung development. The delayed onset of the defect could indicate that the pulmonary defects are secondary to another abnormality, such as an endocrine or metabolic defect. If the effects of the RARβ null mutation were due to a difference in retinoid levels, then one would predict that the body weights of the RARβ null mice would be lower than in the wild-type mice; however, they were not different, except at the 4-wk time point.

Mice in which the RARβ gene had been deleted also had impaired lung function. The decrease in gas exchange surface area uptake in the RARβ gene-deleted mice correlated well with the decrease in lung surface area detected morphometrically, as one would expect for a functional correlate of alveolar gas-exchange surface. There was no difference in the thickness of the alveolar wall in the RARβ gene-deleted mice *versus* the wild-type mice. Therefore, we attribute most of the decrease in gas transfer in the RARβ null mice to the decreased gas-exchange surface area. The uptake of CO is dependent on alveolar ventilation, capillary blood flow, and the diffusion of the gas across the alveolar epithelial-capillary membrane. At resting ventilation, diffusion of CO is not a limiting factor in the transfer of the gas into the blood. At rest, the major factors involved are alveolar ventilation and blood flow. We made an effort to correct partially for differences in alveolar ventilation by normalizing to the exhaled MV, but this did not correct precisely for differences in alveolar ventilation because dead-space ventilation was not excluded. The distribution of dead-space *versus* alveolar ventilation is determined by such factors as airway closure and alveolar recruitment. Although these processes are influenced by the elastic properties of the lung, they are also highly dependent on the physiologic characteristics of the airways. We did not examine changes in the conducting airways in our study, but it is possible that the RARβ null mutation results in changes in the physiologic characteristics of the conducting airways. Alveolar surface area is correlated with the uptake of CO; however, the correlation may not be ideal. During the measurement of CO uptake in our study, the mice were at rest; therefore, their entire alveolar

surface was probably not involved in the exchange of CO. In contrast, the morphometric determination of gas exchange surface area estimated the total surface area and was not influenced by the demand for alveolar ventilation, conducting airway physiology, or alveolar recruitment. Similarly, the surface area measurement was independent of capillary blood flow. It is possible that the surface area abnormality in RARβ null mice may be accompanied by a defect in capillary formation. Abman and co-workers (33,34) reported that treatment of newborn rats with a vascular endothelial growth factor inhibitor decreases blood vessel formation and alveolarization. In summary, there are several unexplored possibilities to explain how the RARβ mutation results in decreased gas-exchange surface area, and we have not yet investigated all of the possible factors.

Mice in which the PDGF-A gene is deleted have impaired postnatal lung alveolarization (24,25). PDGF-A dimers bind to a receptor, PDGF-Rα (24,25). In PDGF-A gene-deleted mice, PDGF-Rα is not expressed in the walls of the prealveolar saccules, and alveolar septation in the postnatal period fails to occur normally (24,25). Thus, there is strong evidence from genetic models that PDGF-A and its receptor may play an important role in postnatal alveolarization. It has been reported that both PDGF-A and PDGF-Rα are regulated by retinoic acid (35–37). Furthermore, it has been shown that retinoic acid stimulates immature lung fibroblast growth *via* PDGF-mediated mechanisms (38). We found that the levels of PDGF-A protein were significantly lower in the lungs of RARβ null mice *versus* those in wild-type control mice. In contrast, the levels of PDGF-Rα mRNA were not different in the two conditions. We examined PDGF-Rα mRNA at several postnatal time points and did not identify a difference between the wild-type and RARβ null animals. Thus, RARβ may regulate alveolarization *via* the PDGF-A/PDGF-Rα axis in the neonatal mouse because a deficiency in PDGF-A has been linked to a profound defect in alveolarization.

Massaro *et al.* (10) reported that the rate of alveolarization is increased in RARβ gene-deleted mice. The RARβ null animals used in the study by Massaro and co-workers (11,27) were generated by deleting exon 10, whereas the RARβ null animals used in the present study were generated by deleting exon 6 of the RARβ gene. In both animal models, however, the expression of RARβ mRNA was ablated. Although the size of the alveoli was decreased and the number of alveoli increased in the studies of Massaro and co-workers, alveolar surface area was not affected by the RARβ null mutation in their study. In contrast, we observed a significant decrease in gas-exchange surface area in the lungs of RARβ null mice at 28, 42, and 56 d postnatal age. A major difference between the morphometric analysis performed by Massaro and co-workers and the present study is that we included alveolar ducts and alveolar sacs in our determination of airspace and tissue volume densities, whereas Massaro and co-workers did not include these structures in their analysis.

We hypothesized that the RARβ gene may affect alveoli and alveolar ducts differently. Alveolar ducts occupy ~33% of the alveolar acinar volume in rats; thus, they make a sizable contribution to the surface area in the distal lung (39). In our study, we found that alveolar ducts and sacs occupy ~37% of the respiratory airspace volume in the mice. It has been proposed that pulmonary alveoli form *via* septation of saccules in the immature lung (40). This process occurs primarily postnatally in mice, rats, and humans (40). We may have detected a decrease in tissue volume density and gas-exchange surface area in the RARβ null mice in the present study because these parameters are derived from alveoli, alveolar sacs, and alveolar ducts. Because alveolar ducts, alveolar sacs, and alveoli all participate in the gas-exchange process, our methods may better predict the physiologic properties of the respiratory unit in the airspace of the distal lung. This is supported by our observation that the ~30% decrease in surface area that we detected morphometrically was accompanied by a similar decrease in CO uptake. It is interesting that Nagai *et al.* (41) showed previously that treatment of postnatal rats with indomethacin, a prostaglandin synthesis inhibitor, results in decreased gas-exchange surface area and an increased volume density of alveolar ducts. Treatment with β-aminopropionitrile, a lysyl oxidase inhibitor, to newborn rats also results in decreased alveoli and an increased volume density of alveolar ducts and sacs (42). Alveolarization, which initially occurs by septation of structures that become the alveolar ducts, is sensitive to the disruption of collagen and elastin synthesis, blood vessel formation, oxygen, and other mediators (43). Thus, the formation and maintenance of alveolar ducts in the neonatal lung is regulated differently than the formation of alveoli. Additional studies directed at understanding the mechanisms of development of the distal lung in RARβ null mice may help further define the role of this gene in the genesis of a normal gas-exchange unit in the lung.

Acknowledgments. We thank Jean Gardner for preparing the manuscript.

REFERENCES

1. Chytil F 1996 Retinoids in lung development. FASEB J 10:986–992
2. Frickel J 1984 Chemistry and physical properties of retinoids. In: Roberts AB, Goodman DS (eds) The Retinoids. Academic Press, Orlando, pp 80–145
3. Chambon P 1996 A decade of molecular biology of retinoic acid receptors. FASEB J 10:940–954
4. Massaro GD, Massaro D 1996 Postnatal treatment with retinoic acid increases the number of pulmonary alveoli in rats. Am J Physiol 270:L305–L310
5. Massaro GD, Massaro D 1997 Retinoic acid treatment abrogates elastase-induced pulmonary emphysema in rats. Nat Med 3:675–677
6. Lucey EC, Goldstein RH, Breuer R, Rexer BN, Ong DE, Snider GL 2003 Retinoic acid does not affect alveolar septation in adult FVB mice with elastase-induced emphysema. Respiration 70:200–205
7. Fujita M, Ye Q, Ouchi H, Nakashima N, Hamada N, Hagimoto N, Kuwano K, Mason RJ, Nakanishi Y 2004 Retinoic acid fails to reverse emphysema in adult mouse models. Thorax 59:224–230
8. McGowan S, Jackson SK, Jenkins-Moore M, Dai HH, Chambon P, Snyder JM 2000 Mice bearing deletions of retinoic acid receptors demonstrate reduced lung elastin and alveolar numbers. Am J Respir Cell Mol Biol 23:162–167
9. Massaro GD, Massaro D, Chambon P 2003 Retinoic acid receptor-alpha regulates pulmonary alveolus formation in mice after, but not during, perinatal period. Am J Physiol 284:L431–L433
10. Massaro GD, Massaro D, Chan WY, Clerch LB, Ghyselinck N, Chambon P, Chandraratna RA 2000 Retinoic acid receptor-beta: an endogenous inhibitor of the perinatal formation of pulmonary alveoli. Physiol Genomics 4:51–57
11. Luo J, Pasceri P, Conlon RA, Rossant J, Giguere V 1995 Mice lacking all isoforms of retinoic acid receptor beta develop normally and are susceptible to the teratogenic effects of retinoic acid. Mech Dev 53:61–71
12. Weibel E 1979 Stereological Methods. Vol 1, Practical Methods for Biological Morphometry. Academic Press, New York
13. Kawakami M, Paul JL, Thurlbeck WM 1984 The effect of age on lung structure in male BALB/cNNia inbred mice. Am J Anat 170:1–21

14. Gundersen HJ, Jensen EB 1987 The efficiency of systematic sampling in stereology and its prediction. J Microsc 147(suppl):229–263
15. Gundersen HJ, Bendtsen TF, Korbo L, Marcussen N, Moller A, Nielsen K, Nyengaard JR, Pakkenberg B, Sorensen FB, Vesterby A, *et al.* 1988 Some new, simple and efficient stereological methods and their use in pathological research and diagnosis. APMIS 96:379–394
16. Zar JH 1984 Biostatistical Analysis. Prentice-Hall, Englewood Cliffs, NJ
17. Schroter RC 1980 Quantitative comparisons of mammalian lung pressure volume curves. Respir Physiol 42:101–107
18. Dekowski SA, Snyder JM 1992 Insulin regulation of messenger ribonucleic acid for the surfactant-associated proteins in human fetal lung in vitro. Endocrinology 131:669–676
19. Chen H, Jackson S, Doro M, McGowan S 1998 Perinatal expression of genes that may participate in lipid metabolism by lipid-laden lung fibroblasts. J Lipid Res 39:2483–2492
20. McGowan SE, Harvey CS, Jackson SK 1995 Retinoids, retinoic acid receptors, and cytoplasmic retinoid binding proteins in perinatal rat lung fibroblasts. Am J Physiol 269:L463–L472
21. Bradford MM 1976 A rapid and sensitive method for the quantitation of microgram quantities of protein utilizing the principle of protein-dye binding. Anal Biochem 72:248–254
22. George TN, Snyder JM 1997 Regulation of surfactant protein gene expression by retinoic acid metabolites. Pediatr Res 41:692–701
23. Amy RW, Bowes D, Burri PH, Haines J, Thurlbeck WM 1977 Postnatal growth of the mouse lung. J Anat 124:131–151
24. Bostrom H, Willetts K, Pekny M, Leveen P, Lindahl P, Hedstrand H, Pekna M, Hellstrom M, Gebre-Medhin S, Schalling M, Nilsson M, Kurland S, Tornell J, Heath JK, Betsholtz C 1996 PDGF-A signaling is a critical event in lung alveolar myofibroblast development and alveogenesis. Cell 85:863–873
25. Lindahl P, Karlsson L, Hellstrom M, Gebre-Medhin S, Willetts K, Heath JK, Betsholtz C 1997 Alveogenesis failure in PDGF-A-deficient mice is coupled to lack of distal spreading of alveolar smooth muscle cell progenitors during lung development. Development 124:3943–3953
26. Chambon P 1995 The molecular and genetic dissection of the retinoid signaling pathway. Recent Prog Horm Res 50:317–332
27. Ghyselinck NB, Dupe V, Dierich A, Messaddeq N, Garnier JM, Rochette-Egly C, Chambon P, Mark M 1997 Role of the retinoic acid receptor β (RARβ) during mouse development. Int J Dev Biol 41:425–447
28. Mendelsohn C, Lohnes D, Decimo D, Lufkin T, LeMeur M, Chambon P, Mark M 1994 Function of the retinoic acid receptors (RARs) during development (II). Multiple abnormalities at various stages of organogenesis in RAR double mutants. Development 120:2749–2771
29. Underhill TM, Kotch LE, Linney E 1995 Retinoids and mouse embryonic development. Vitam Horm 51:403–457
30. Mollard R, Ghyselinck NB, Wendling O, Chambon P, Mark M 2000 Stage-dependent responses of the developing lung to retinoic acid signaling. Int J Dev Biol 44:457–462
31. Hind M, Corcoran J, Maden M 2002 Temporal/spatial expression of retinoid binding proteins and RAR isoforms in the postnatal lung. Am J Physiol 282:L468–L476
32. Yang L, Naltner A, Yan C 2003 Overexpression of dominant negative retinoic acid receptor alpha causes alveolar abnormality in transgenic neonatal lungs. Endocrinology 144:3004–3011
33. Jakkula M, Le Cras TD, Gebb S, Hirth KP, Tuder RM, Voelkel NF, Abman SH 2000 Inhibition of angiogenesis decreases alveolarization in the developing rat lung. Am J Physiol 279:L600–L607
34. Le Cras TD, Markham NE, Tuder RM, Voelkel NF, Abman SH 2002 Treatment of newborn rats with a VEGF receptor inhibitor causes pulmonary hypertension and abnormal lung structure. Am J Physiol 283:L555–L562
35. Afink GB, Nister M, Stassen BH, Joosten PH, Rademakers PJ, Bongcam-Rudloff E, Van Zoelen EJ, Mosselman S 1995 Molecular cloning and functional characterization of the human platelet-derived growth factor alpha receptor gene promoter. Oncogene 10:1667–1672
36. Mummery CL, van den Eijnden-van Raaij AJ, Feijen A, Freund E, Hulskotte E, Schoorlemmer J, Kruijer W 1990 Expression of growth factors during the differentiation of embryonic stem cells in monolayer. Dev Biol 142:406–413
37. Wang C, Kelly J, Bowen-Pope DF, Stiles CD 1990 Retinoic acid promotes transcription of the platelet-derived growth factor alpha-receptor gene. Mol Cell Biol 10:6781–6784
38. Liebeskind A, Srinivasan S, Kaetzel D, Bruce M 2000 Retinoic acid stimulates immature lung fibroblast growth via a PDGF-mediated autocrine mechanism. Am J Physiol 279:L81–L90
39. Randell SH, Mercer RR, Young SL 1990 Neonatal hyperoxia alters the pulmonary alveolar and capillary structure of 40-day-old rats. Am J Pathol 136:1259–1266
40. Massaro D, Massaro GD 2002 Pre- and postnatal lung development, maturation, and plasticity invited review: pulmonary alveoli: formation, the "call for oxygen," and other regulators. Am J Physiol 282:L345–L358
41. Nagai A, Katayama M, Thurlbeck WM, Matsui R, Yasui S, Konno K 1995 Effect of indomethacin on lung development in postnatal rats: possible role of prostaglandin in alveolar formation. Am J Physiol 268:L56–L62
42. Kida K, Thurlbeck WM 1980 The effects of beta-aminopropionitrile on the growing rat lung. Am J Pathol 101:693–710
43. Snyder JM 2004 Regulation of alveolarization. In: Polin RA, Fox WW, Abman S (eds) Fetal and Neonatal Physiology. Saunders, Philadelphia, pp 794–801